Accuracy assessment of Copernicus program 2012 High-Resolution Layers for Continental Portugal

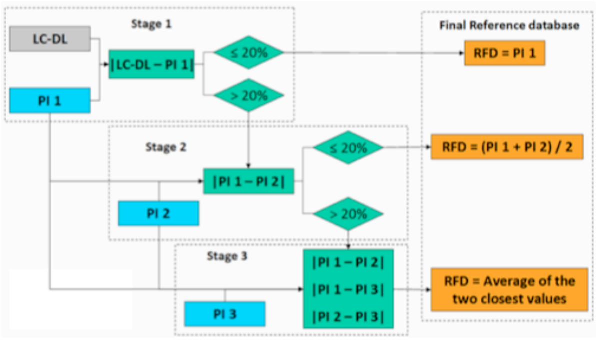

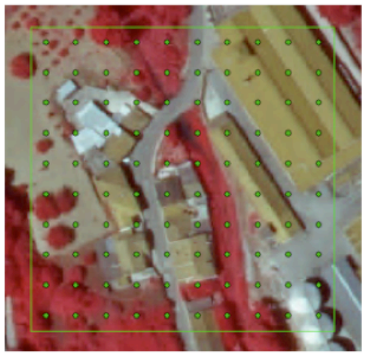

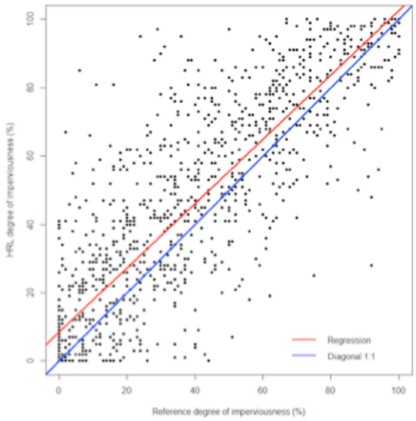

Pedro Sarmento, Filipe Marcelino, Giselda Monteiro, Jonas Schmedtmann and Mário Caetano

November, 2015

European Environment Agency

Executive summary

This document presents the accuracy assessment of three 2012 High-Resolution Layers (HRLs) produced by the European Environmental Agency (EEA) under the GMES/Copernicus Initial Operations (GIO) Land Monitoring 2011-2013 for Continental Portugal. These HRLs are described in Marcelino et al. (2015) and the three ones that are assessed here are: Degree of Imperviousness, Tree Cover Density and Forest Type. The accuracy assessment was performed on the 100 m products that were derived from the 20 m products (intermediate products).

The sampling units were selected through a stratified random sampling. The sample size for the continuous products is 1200 and for the Forest Type is 1400. The reference data was collected over aerial images with 0,4 m of spatial resolution and in order to reduce subjectivity many sampling unit were visited by more than one photo-interpreter. The accuracy assessment of the continuous layers was based on Pearson correlation coefficient (r), coefficient of determination (r^2), mean absolute error (MAE) and root mean square error (RMSE). The accuracy assessment of the Forest Type HRL takes into account the abundance of each class and is based on overall accuracy and user's and producer's accuracies.

Both continuous products, i.e. Degree of Imperviousness and Tree Cover Density, are very good, with a mean absolute error of 12% and 14%, respectively. There is some overestimation of the degree of imperviousness value for the Degree of Imperviousness HRL and some underestimation of the tree cover density values for the Tree Cover Density HRL.

Overall accuracy of the Forest type HRL was estimated at 79,7% with an absolute precision of 2,2% at the 95% confidence level. However there are some important differences in the accuracies of the four classes, which in some cases the accuracies are very low. The All non-forest areas class has very good user's and producer's accuracy (84.4% and 95.2%). The user's accuracies of Broadleaf, Coniferous and Mixed forests are 73.0%, 64.0% and 29.5%. The producer's accuracies of Broadleaf, Coniferous and Mixed forests are 56.3%, 41.4% and 24.8%.

Index

Table index

Figure index

List of symbols, abbreviations and acronyms

d	Absolute precision
DGT	Directorate General for Territory Development
EEA	European Environmental Agency
FAO	Food and Agriculture Organization of the United Nations
GIO	GMES/Copernicus Initial Operations
GMES	Global Monitoring for Environment and Security
HRL	High Resolution Layer
LC-DL	Land Cover Density Layer
LC-TLs	Land Cover Thematic Layer
MAE	Mean absolute error
n	Number of sample observations
n_g	Number of sample observations per reference class
N_g	Area occupied per reference class
n_h	Number of sample observations per map class
N_h	Area occupied per map class
NRC	National Reference Centre
P	Overall accuracy
P_g	Producer's accuracy
P_h	User's accuracy
r	Pearson correlation
r^2	Coefficient of determination
RMSE	Root mean square error

1 Introduction

The purpose of this document is to present the accuracy assessment of three 2012 High-Resolution Layers (HRLs) produced by the European Environmental Agency (EEA) under the GMES/Copernicus Initial Operations (GIO) Land Monitoring 2011-2013 for Continental Portugal. These HRLs are described in Marcelino et al. (2015).

The accuracy assessment of the HRLs was performed according to the characteristics of the data. There are two types of HRLs:

- Land Cover Density Layers (LC-DLs) - HRLs with continuous data, i.e. Degree of Imperviousness and Tree Cover Density;
- Land Cover Thematic Layers (LC-TLs) - HRLs with categorical data, i.e. Forest Type.

The accuracy assessment was performed on the HRLs final product (i.e. the products with 100 m of spatial resolution). We only validated the following HRLs: Degree of Imperviousness, Tree Cover Density and Forest Type.

This document is divided into five sections. The HRLs technical specifications are presented in Section 2. In Section 3 the accuracy assessment protocol is presented, followed by the results of the accuracy assessment in Section 4. In Section 5 the main conclusions of the accuracy assessment of the HRLs are presented.

2 HRLs definition and technical specifications

The definition and the main technical specifications of the HRLs are presented in Table 1. The accuracy assessment was performed on the 100 m products that were derived from the 20 m products (intermediate products).

Table 1. HRLs definition and technical specifications.

HRLs		Definition	Geometric resolution	Projection	Minimum mapping unit	Classified feature	Raster coding
Land Cover Density Layers	Degree of Imperviousness 2012	This product maps the covering of the soil surface with impervious materials as a result of urban development and infrastructure construction	100 m	ETRS 89 PORTUGAL TM06	no	Degree of imperviousness (1%-100%)	0: all non-impervious areas 1-100: imperviousness values 254:unclassifiable 255: outside area
	Tree Cover Density 2012	This product maps the tree cover range (1%-100%) with a minimum mapping width of 20m	100 m	ETRS 89 PORTUGAL TM06	no	Tree cover density (1%-100%)	0: all non-tree areas 1-100: tree cover density 254: unclassifiable 255: outside area
Land Cover Thematic Layers	Forest Type 2012	This product maps the forest type more closely aligned to the FAO forest definition	100 m	ETRS 89 PORTUGAL TM06	no	Broadleaf forest, Coniferous forest, Mixed forest	0: all non-forest areas 1: broadleaf forest 2: coniferous forest 3: mixed forest 254: unclassifiable 255: outside area

3 Accuracy assessment protocol

According to Stehman and Czaplewski (1998) an accuracy assessment should entail three basic components: (1) the sampling design; (2) the response design; and (3) the estimation and analysis procedures. In the present section, the proposed methodology to perform the accuracy assessment of the HRLs in each one of these three basic components is presented.

3.1 Sampling design

The sampling design is the protocol by which the reference sample units are selected (Stehman and Czaplewski 1998). Choosing a probability sampling design requires the choice of a sampling unit and also the sampling protocol, which form the basis of an accuracy assessment.

3.1.1 Sampling unit

The accuracy assessment of the HRLs was performed at the spatial resolution of the final product (i.e. 100 m). The comparison between the HRLs and the reference database was made on *a per* pixel basis and the sampling unit had the dimension of a pixel of 1ha.

3.1.2 Sampling protocol

Sampling is the protocol in which the sampling units are selected (Stehman and Czaplewski 1998). In order to guarantee a good precision of the accuracy estimation, a stratified random sampling was used to select the sampling units. Using a stratified random sampling to select the sampling units guarantees a better distribution over the continuous values of the LC-DLs. This aspect is important for example to determine the accuracy of the Degree of Imperviousness. Because the impervious surfaces are concentrated in urban areas, and these occupy small areas when compared with the non-imperviousness areas, if a simple random sampling was used, this would result in an underestimation of the sample size for the pixels with high values of imperviousness.

Using a stratified random sampling is also important to guarantee that categorical classes of the LC-TLs that are less represented in the HRL have an adequate number of sample observations (e.g. Mixed forest of the Forest Type HRL).

3.1.3 Sample size

For a statistically valid accuracy assessment, the collection of an adequate number of sampling units for each class is necessary (Congalton and Green 1999). The sample size was computed according to the equation proposed by Carrão et al. (2007). A sample size of 200 sample observations was used for each HRL class, regarding a target accuracy of 85% for each HRL, with a confidence level of 95% and with a maximum error of 5%. Additional 600 sample observations were selected for the stratum of All non-forest areas class of the Forest type HRL in order to detect more possible omission errors, because this land cover class occupies a very large area of the Continental Portugal territory.

Table 2 shows the sample size defined for each stratum and also the total sample size for each HRL.

Table 2. Sample size for each stratum (n_h) and total sample size (n) for each HRL.

HRL	Stratum (h)	Number of sample observations per stratum (n_h)	Sample size (n)
Degree of imperviousness and Tree cover density	0 %	200	1200
	[1% - 20%[	200	
	[20% - 40%[	200	
	[40% - 60%[	200	
	[60% - 80%[	200	
	[80% - 100%]	200	
Forest type	All non-forest areas	800	1400
	Broadleaf forest	200	
	Coniferous forest	200	
	Mixed forest	200	

3.2 Response design

The response design defines the protocol for determining the ground condition (i.e. the reference classification) at the selected sampling units (Olofsson et al. 2012). The response design is divided in two components: (1) the evaluation protocol; and (2) the labelling protocol.

3.2.1 Evaluation protocol

The evaluation protocol consists in choosing the spatial support region that will be analyzed to collect the reference data. The spatial support region was defined accordingly with the specific geometric resolution of the LC-DLs and the LC-TL (i.e. an area of 100 m x 100 m).

3.2.2 Labelling protocol

In the labelling protocol the reference classification is assigned to the sampling unit based on the information that is collected, analyzing the spatial support region.

The procedure for collecting the reference data consisted in photo-interpretation of aerial images acquired during 2012 covering the whole Portuguese territory. These images have four spectral bands (blue, green, red, and near-infrared) and 0,4 m of spatial resolution.

The photo-interpretation was performed at a scale of 1:1000, for the sampling units of each HRL. The labelling protocol for collecting the reference data was divided in several stages, and the sampling units were visited by more than one photo-interpreter in order to reduce subjectivity. In each one of these stages, additional photo-interpreter(s) collected the reference data, and the sampling units that were added to the different stages were selected according to a set of rules that are explained further below for each HRL data type (i.e. LC-DLs and LC-TL).

Land Cover Density Layers labelling protocol

Stage 1

- At each sample observation, photo-interpreter 1 classified the degree of imperviousness (0-100%) (in the case of the Degree of Imperviousness HRL) and the tree cover (0-100%) (in the case of the Tree Cover Density HRL) that exists in the sampling unit without prior knowledge of the HRL classification. This is done by means of counting a systematically aligned set of 100 points overlaid over each sampling unit. For each one of these 100 points the photo-interpreters determined a binary imperviousness state (i.e. impervious or not impervious) in the case of the Degree of Imperviousness density HRL, and a binary tree cover state (i.e. with tree cover or not tree cover) in the case of the Tree Cover Density HRL. For example, counting the number of points falling in impervious areas inside the sampling units could be assigned the reference degree of imperviousness (Figure 1). The same rationale is applied to the tree cover areas, but in this case by counting the points that fall in tree canopies (Figure 1). This method to determine the density values within each sampling unit was also applied in other studies (Nowak et al. 1996; Greenfield et al. 2009; Knight and Voth, 2011).

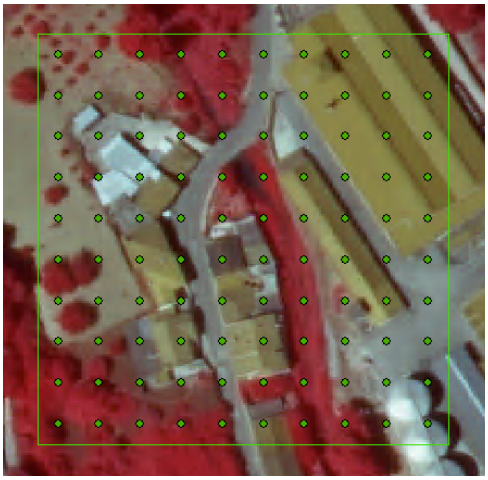

Figure 1. A set of 100 points systematically distributed over a sampling unit.

- The sampling units wherein the absolute difference between the LC-DL classification and the photo-interpreted classification was larger than 20%, were selected to be photo-interpreted by a second photo-interpreter in Stage 2. The sampling units wherein the absolute difference between the LC-DL classification and the photo-interpreted classification was smaller or equal to 20% were considered final and added to the final reference database.

Stage 2

- The collection of the reference data by photo-interpreter 2 was made accordingly with the method previously described in Stage 1. At this stage, the sampling units wherein the absolute difference between photo-interpreter 1 classification and photo-interpreter 2 classification was larger than 20% were selected to be photo-interpreted by a third photo-interpreter in Stage 3. The sampling units wherein the absolute difference between photo-interpreter 1 classification and photo-interpreter 2 classification was smaller or equal to 20% were selected and the mean classification value between photo-interpreters was computed. This mean value was considered final and added to the final reference database.

Stage 3

- The collection of the reference data by photo-interpreter 3 was made accordingly with the method previously described in Stage 1. The classification between the three photo-interpreters was compared and the final classification value was considered the mean between the two closest classification values between two of the three photo-interpreters. This mean value was considered final and added to the final reference database. Table 3 shows the number of sample observations in each stage of the LC-DLs labelling protocol.

Table 3. Number of sample observation in each stage of the LC-DLs labelling protocol.

Land Cover Density Layer	Stage 1 (*n*)	Stage 2 (*n*)	Stage 3 (*n*)
Degree of Imperviousness	1200	284	24
Tree Cover Density	1200	450	150

Figure 2 shows the labelling protocol flowchart along the three stages of the labelling protocol of the LC-DLs.

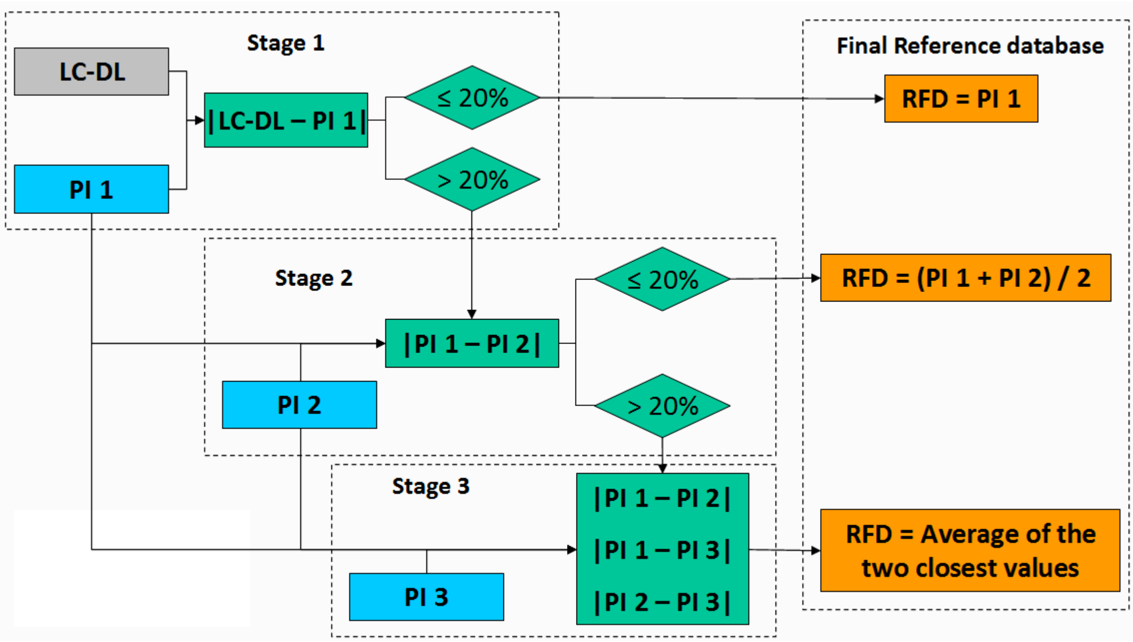

Figure 2. LC-DLs labelling protocol flowchart, where: PI 1: photo-interpreter 1; PI 2: photo-interpreter 2; PI 3: photo-interpreter 3 and RFD: reference database.

<u>Land Cover Thematic Layer labelling protocol</u>

Stage 1

- Photo-interpreter 1 classified each sample observation with the land cover class that best describes the location of the sampling unit according with the land cover classes of the LC-TL (i.e. Forest Type HRL), without prior knowledge of the HRL classification. After the collection of the reference data for all sampling units, the reference classification was compared with the LC-TL classification. The sampling units where the reference classification matched the LC-TL classification were considered final and added to the final reference database. On the other hand, the sampling units where the reference classification did not matched the LC-TL classification were selected to be photo-interpreted by a second and a third photo-interpreter (photo-interpreter 2 and photo-interpreter 3) in Stage 2.

Stage 2

- The collection of the reference data by photo-interpreter 2 and photo-interpreter 3 in the sampling units that were selected in Stage 1, was performed with the same approach as described in Stage 1. The sampling units where the reference classification of photo-interpreter 2 or photo-interpreter 3 matched the reference classification of photo-interpreter 1, and also the sampling units where the reference classification of photo-interpreter 2 matched the reference classification of photo-interpreter 3 were considered final and added to the final reference database. The sampling units where the reference classification between the three photo-interpreters didn't matched were selected to be photo-interpreted by two additional photo-interpreters (photo-interpreter 4 and photo-interpreter 5) in Stage 3.

Stage 3

- The collection of the reference data by photo-interpreter 4 and photo-interpreter 5 in the sampling units that were selected in Stage 2 was performed with the same approach as described in Stage 1. The sampling units where a match of the reference classification was found, for at least three photo-interpreters, were considered final and added to the final reference database. The sampling units where a match just between two photo-interpreters was found were selected to be photo-interpreted by an additional photo-interpreter (photo-interpreter 6) in Stage 4.

Stage 4

- The collection of the reference data by photo-interpreter 6 in the sampling units that were selected in Stage 3 was performed with the same approach as described in Stage 1. The sampling units where a match of the reference classification was found, for at least three photo-interpreters, were considered final and added to the final reference database.

Table 4 shows the number of sample observations in each stage of the LC-TL labelling protocol.

Table 4. Number of sample observation in each stage of the LC-TL labelling protocol.

Land Cover Thematic Layer	Stage 1 (*n*)	Stage 2 (*n*)	Stage 3 (*n*)	Stage 4 (*n*)
Forest Type	1400	484	31	6

Figure 3 shows the labelling protocol flowchart along the three stages of the collection of the reference data.

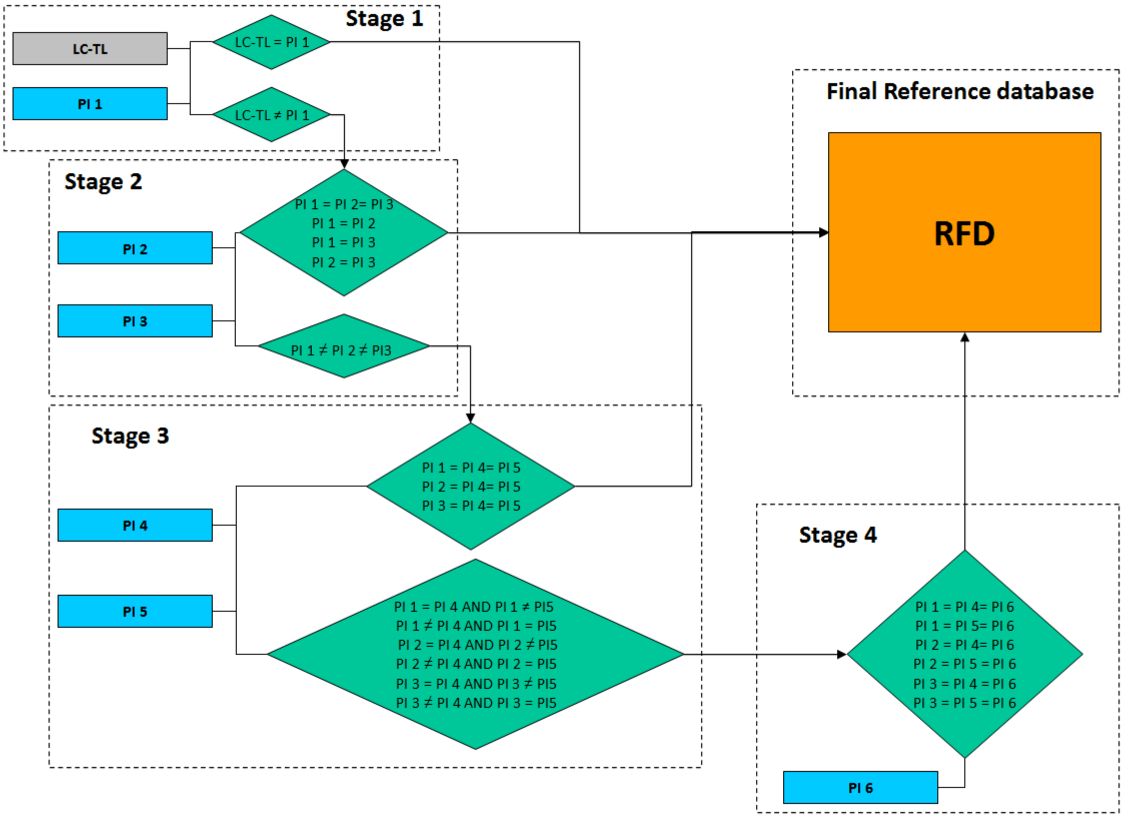

Figure 3. LC-TL labelling protocol flowchart, where: PI 1: photo-interpreter 1; PI 2: photo-interpreter 2; PI 3: photo-interpreter 3; PI 4: photo-interpreter 4; PI 5: photo-interpreter 5; PI 6: photo-interpreter 6 and RFD: reference database.

3.3 Estimation and analysis

The LC-DLs accuracy was computed and analyzed using several estimators that are widely used in the accuracy assessment of continuous variables, namely: (1) a scatter plot (Dougherty et al. 2004; Greenfield et al. 2009; Lu and Weng 2006; Wu and Yuan 2007); (2) Pearson correlation coefficient (*r*) (Dougherty et al. 2004; Greenfield et al. 2009; Homer et al. 2004; Mohapatra and Wu, 2010); (3) Coefficient of determination (r^2) (Dougherty et al. 2004; Hu and Weng, 2009; Weng and Hu, 2008; Wu and Yuan, 2007); (4) mean absolute error (MAE) (Homer et al. 2004; Hu and Weng, 2009; Long II et al. 2013; Mohapatra and Wu, 2010; Wu and Yuan, 2007); and (5) root mean square error (RMSE) (Deng et al. 2012; Hu and Weng, 2009; Long II et al. 2013; Weng and Hu, 2008). In Table 5 is presented the meaning of these estimators.

Table 5. Estimators computed for the accuracy assessment of the LC-DLs.

Estimator	Meaning
Pearson correlation (*r*)	Measure of linear correlation between two variables ($-1 \leq r \leq 1$). -1: Total negative correlation 1: Total positive correlation 0: No correlation
Coefficient of determination (r^2)	Measure of how well observed values are replicated by the linear regression ($0 \leq r^2 \leq 1$) 0: The regression line doesn't fit the data 1: The regression line fits perfectly the data
Mean absolute error (MAE)	Measure of the differences between the estimated and the observed values.
Root mean square error (RMSE)	Measure of the difference between the estimated and the observed values. Accentuate the effect of large errors.

To derive the accuracy of the LC-TL an error matrix was elaborated. Through the error matrix it was possible to derive the user's accuracy (commission errors) and the producer's accuracy (omission errors) as well the overall accuracy of the LC-TL. The error matrix has been in the core of other accuracy assessment studies (Stehman et al. 2003; Wickham et al. 2004; Wickham et al. 2013).

The accuracy assessment of the LC-TL was conducted elaborating a map error matrix where the area of each map class is accounted in the accuracy assessment. Card (1982) stated that for the stratified sampling case, the overall proportion of correctly classified individuals should not be simply estimated by the diagonal entry divided by the row sum of the error matrix, because of the bias introduced by possible differential sampling rates within map categories. Therefore, the overall and per class accuracy estimations should include the known areas of each map class to improve the estimation of the proportion of correctly mapped individuals. To derive the specific and overall accuracy as well their precision we used the equations proposed by Carrão et al. (2007) which follows the recommendations of Card (1982).

4 Results

4.1 Land Cover Density Layers

4.1.1 Degree of Imperviousness

Table 6 and Figure 4 show the accuracy assessment results for the Degree of Imperviousness HRL.

Table 6. Accuracy assessment estimators computed for the Degree of Imperviousness HRL.

Estimator	Value
Pearson correlation (*r*)	0,87
Coefficient of determination (r^2)	0,75
Mean absolute error (MAE)	12%
Root mean square error (RMSE)	18%

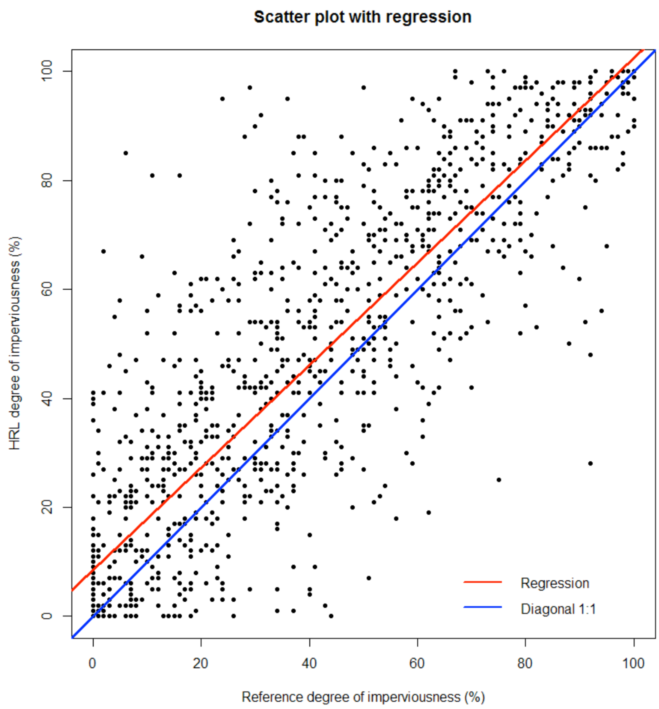

Figure 4. Scatter plot of the Degree of Imperviousness along with linear regression (red) and line (blue) indicating a 1:1 relationship between the HRL Degree of Imperviousness and the photo-interpreted degree of imperviousness.

The value obtained for *r* indicates a strong positive relationship between the HRL Degree of Imperviousness values and the photo-interpreted degree of imperviousness values, while r^2 indicates a correlation of 0,75 between the HRL Degree of Imperviousness values and the photo-interpreted degree of imperviousness values. MAE and RMSE are respectively 12% and 18%.

Figure 5 shows the residuals plot (differences between Degree of Imperviousness HRL and photo-interpreted degree of imperviousness) for the Degree of imperviousness HRL.

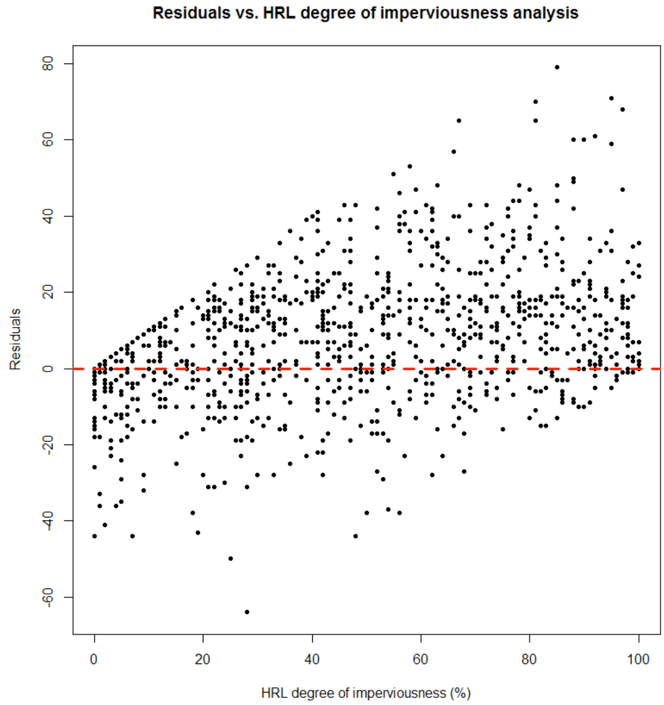

Figure 5. Residuals plot for the Degree of Imperviousness HRL.

Analyzing Figure 5, it can be stated that the majority of the point cloud is above the red line (where the difference between Degree of Imperviousness HRL and photo-interpreted degree of imperviousness equals 0) indicating that an overestimation of the degree of imperviousness values in the HRL exists.

4.1.2 Tree Cover Density

Table 7 and Figure 6 show the accuracy assessment results for the Tree Cover Density HRL.

Table 7. Accuracy assessment estimators computed for the Tree Cover Density HRL.

Estimator	Value
Pearson correlation (*r*)	0,79
Coefficient of determination (r^2)	0,63
Mean absolute error (MAE)	14%
Root mean square error (RMSE)	20%

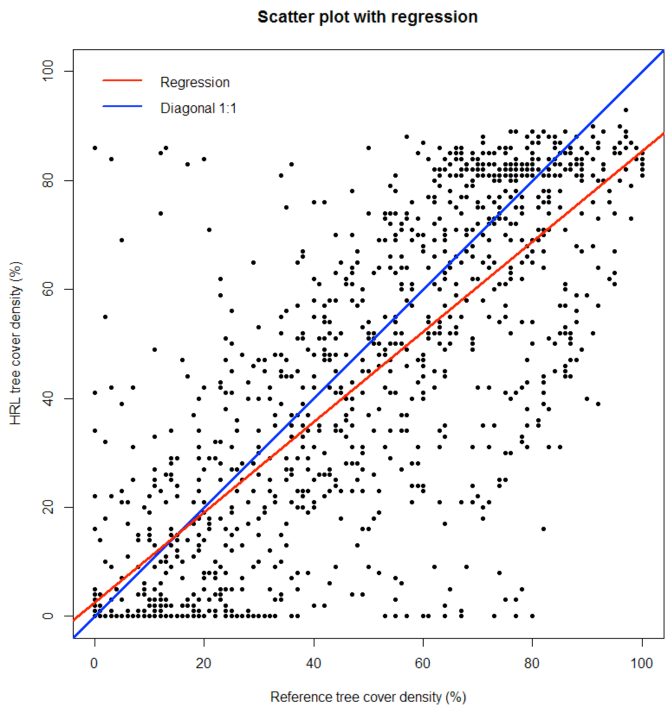

Figure 6. Scatter plot of the Tree Cover Density along with linear regression (red) and line (blue) indicating a 1:1 relationship between the HRL Tree Cover Density and the photo-interpreted tree cover density.

The value obtained for r indicates a moderate positive relationship between the Tree Cover Density HRL values and the photo-interpreted tree cover density values, while r^2 indicates a correlation of 0,63 between the Tree Cover Density HRL values and the photo-interpreted tree cover density values. MAE and RMSE are respectively 14% and 20%.

Figure 7 shows the residuals plot (difference between Tree Cover Density HRL and photo-interpreted tree cover density equals 0) for the Tree Cover Density HRL.

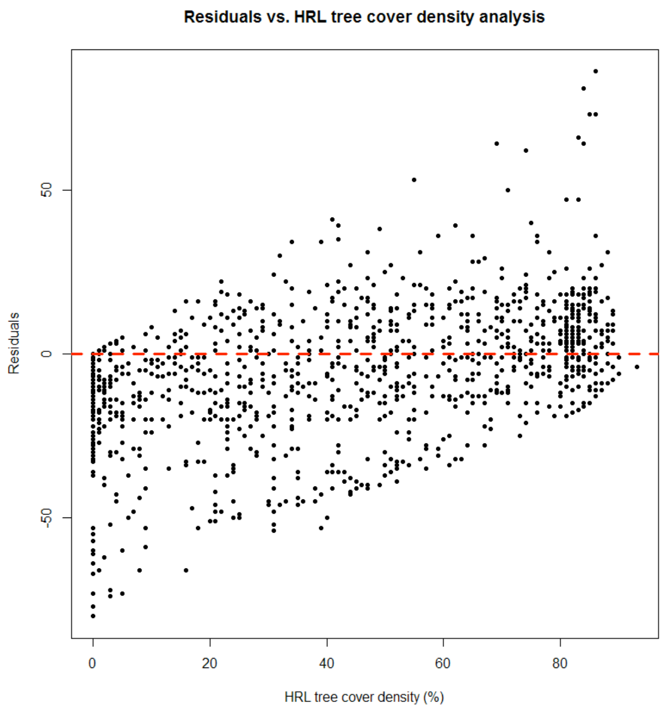

Figure 7. Residuals plot for the Tree Cover Density HRL.

Analyzing Figure 7, it could be stated that the majority of the point cloud is under the red line (where the difference between Tree Cover Density HRL and photo-interpreted tree cover density equals 0) indicating that an underestimation of the tree cover density values in the HRL exists.

4.2 Land Cover Thematic Layer

4.2.1 Forest Type

Table 8 presents the percentage of area occupied per mapped land cover class (N_h), and the 95% confidence intervals for the percentage of area occupied per reference land cover class (N_g), overall accuracy (P), user's accuracy (P_h), producer's accuracy (P_g) and the absolute precisions estimated for a 95% confidence level for P, P_h and P_g ($d(P)$, $d(P_h)$ and $d(P_g)$). An estimated map error matrix was also computed (Table 9), where the values inside the error matrix represent the percentage of matches between map and reference land cover classes as a percentage of the total Forest type HRL area.

Table 8 – Percentage of area occupied per mapped land cover class (N_h), and 95% confidence intervals for percentage of area occupied per reference land cover class (N_g), overall accuracy (P), user's accuracy (P_h) and producer's accuracy (P_g). Absolute precision is represented by d.

Land cover class	N_h	$N_g \in [\hat{N}_g - d(\hat{N}_g);\ \hat{N}_g + d(\hat{N}_g)]$	$P_h \in [\hat{P}_h - d(\hat{P}_h);\ \hat{P}_h + d(\hat{P}_h)]$	$P_g \in [\hat{P}_g - d(\hat{P}_g);\ \hat{P}_g + d(\hat{P}_g)]$
All non-forest areas	75,1	[65,7; 67,3]	[81,9; 86,9]	[94,0; 96,4]
Broadleaf forest	15,9	[18,4; 23,0]	[66,8; 79,2]	[51,6; 61,0]
Coniferous forest	5,9	[6,5; 11,7]	[57,3; 70,7]	[35,3; 47,5]
Mixed forest	3,1	[0,0; 7,1]	[23,2; 35,8]	[17,8; 31,8]
Overall accuracy		$P \in [\hat{P} - d(\hat{P});\ \hat{P} + d(\hat{P})]$	[77,5; 81,9]	

Table 9. Estimated map error matrix, where values inside the map error matrix represent the estimated percentage of matches between the Forest Type HRL and reference land cover classes as a percentage of the total Forest type HRL area.

		Reference data						
		All non-forest areas	Broadleaf forest	Coniferous forest	Mixed forest	N_h (%)	P_h (%)	$d(P_h)$ (%)
Forest type HRL	All non-forest areas	63,3	7,1	3,4	1,2	75,1	84,4	2,5
	Broadleaf forest	2,5	11,6	1,1	0,7	15,9	73,0	6,2
	Coniferous forest	0,4	0,8	3,8	0,9	5,9	64,0	6,7
	Mixed forest	0,3	1,1	0,8	0,9	3,1	29,5	6,3
N_g (%)		66,5	20,7	9,1	3,7	100	P	$d(P)$
P_g (%)		95,2	56,3	41,4	24,8		79,7	2,2
$d(P_g)$ (%)		1,2	4,7	6,1	7,0			

Overall accuracy of the Forest Type HRL was estimated at 79,7% with an absolute precision of 2,2% at the 95% confidence level.

Regarding the All non-forest areas class user's accuracy was estimated at 84,4%. The major percentage of mismatches of the All non-forest areas class occurred in the Broadleaf forest class (7,1%). The user's accuracy of the Broadleaf forest class was estimated at 73% and the major part of the mismatches occurred in the All non-forest areas class (2,5%). Coniferous forest class achieved an acceptable value of accuracy, corresponding to 64%. The major mismatches of the Coniferous forest class occurred in a similar percentage with the Broadleaf forest class (0,8%) and the Mixed forest class (0,9%). With a very low value of user's accuracy, the Mixed forest class presented the lowest value of user's accuracy between all the land cover classes of the Forest Type HRL. The mismatches occurred in a similar percentage between the Broadleaf forest class (1,1%) and the Coniferous forest class (0,8%).

The producer's accuracy of all forest type land cover classes is relatively low, excepting the All non-forest areas class (95,2%). This aspect could be explained by the major difference in reference class areas (All non-forest areas class represents N_g=66,5%) and the high proportion of matches for the All non-forest areas class (63,3%). Indeed analyzing the mismatches by column for the forest land cover classes it could be stated that the major proportion of mismatches occurred with the All non-forest areas class (7,1% for the Broadleaf forest class, 3,4% for the Coniferous forest class and 1,2% for the Mixed forest class). This aspect is associated with the large area occupied in the map by the All non-forest areas class and explains the low values of producer's accuracy for these forest land cover classes.

Another important aspect that could be retained analyzing the error matrix is that the Forest type HRL overestimates the area of All non-forest areas (for the All non-forest areas class N_h=75,1% while N_g=66,5%) and consequently the Forest type HRL underestimates the remaining forest land cover classes (N_g is always superior when compared with N_h for the Broadleaf forest class, Coniferous forest class and Mixed forest class).

5 Conclusion

This report describes the accuracy assessment protocol of the 2012 High-Resolution Layers for Continental Portugal.

The accuracy of the Land Cover Density Layers (LC-DLs) is very good, with a mean absolute error of 12% for the Degree of Imperviousness HRL and 14% for the Tree Cover Density HRL. However, through the analysis of the residuals plots for both products it was stated that exists an overestimation of the degree of imperviousness values and an underestimation of the tree cover density values.

Regarding the Land Cover Thematic Layers (LC-TL) (i.e. Forest type) accuracy assessment, the overall accuracy obtained was high (79,7%). The high presence of the All non-forest areas class in the map affects the producer's accuracy of the Broadleaf forest class, Coniferous forest class and Mixed forest class (56,3%, 41,4% and 24,8% respectively).

Despite the good overall accuracy of the Forest Type HRL there were some important differences in the accuracy of the individual land cover classes. For example, the All non-forest areas class and Broadleaf forest class achieved good values of user's accuracy (84,4% and 73% respectively) while the Coniferous forest achieved an acceptable level of accuracy user's accuracy (64%). The user's accuracy for the Mixed forest class was very low (29,5%) and this class should be used with caution in any application that uses this information.

Through the analysis of the map error matrix we also concluded that exists an overestimation of the All non-forest areas class of the Forest type HRL (N_h = 75,1% and N_g = 66,5%) and consequently an underestimation of the forest classes (the N_h value is always inferior to N_g value for the Broadleaf forest class, Coniferous forest class and the Mixed forest class).

References

Card, G., 1982. Using known map category marginal frequencies to improve estimates of thematic map accuracy, Photogrammetric Engineering & Remote Sensing, 48: 431-439.

Carrão, H., M. Caetano, and P. Coelho, 2007. Sample Design and Analysis for Thematic Map Accuracy Assessment: An Approach Based on Domain Estimation for the Validation of Land Cover Products, Proceedings of the 32nd International Symposium on Remote Sensing of Environment, 25-29 June 2007, San José, Costa Rica.

Congalton, R., and K. Green, 1999. Assessing the Accuracy of Remotely Sensed Data: Principles and Practices, CRC/Lewis Press, Boca Raton, Florida.

Deng, Y., F. Fan, and R. Chen, 2012. Extraction and Analysis of Impervious Surfaces Based on a Spectral Un-Mixing Method Using Pearl River Delta of China Landsat TM/ETM+ Imagery from 1998 to 2008, Sensors, 12: 1846-1862.

Dougherty, M., R. L. Dymond, S. J. Goetz, C. A. Jantz, and N. Goulet, 2004. Evaluation of Impervious Surface Estimates in a Rapidly Urbanizing Watershed, Photogrammetric Engineering & Remote Sensing, 70(11): 1275-1284.

Greenfield, E. J., D. J. Nowak, and J. T. Walton, 2009. Assessment of 2001 NLCD Percent Tree and Impervious Cover Estimates, Photogrammetric Engineering & Remote Sensing, 75(11): 1279-1286.

Homer, C., C. Huang, L. Yang, B. Wylie, M. Coan, 2004. Development of a 2001 National Land-Cover Database for the United States, Photogrammetric Engineering & Remote Sensing, 70(7): 829-840.

Hu, X., and Q. Weng, 2009. Estimating impervious surfaces from medium spatial resolution imagery using self-organizing map and multi-layer perceptron neural networks, Remote Sensing of Environment, 113: 2089-2102.

Knight, J., and M. Voth, 2011. Mapping Impervious Cover Using Multi-Temporal MODIS NDVI Data, IEEE Journal of Selected Topics in Applied Earth Observations and Remote Sensing, 4(2): 303-309.

Long II, D. E., J. D. Carr, H. O. Liechty, and H. C. Stuhlinger, 2013. Accuracy Assessment of the 2006 National Land Cover Database Percent Impervious Cover, Journal of the Arkansas Academy of Science, 67: 81-86.

Lu, D., and Q. Weng, 2006. Use of impervious surface in urban land-use classification, Remote Sensing of Environment, 102: 146-160.

Marcelino, F., P. Sarmento, G. Monteiro, and M. Caetano, 2015. Temas de Alta Resolução (HRLs) do programa *Copernicus* para Portugal Continental, Relatório técnico, DGT.

Mohapatra, R. P., and C. Wu, 2010. High Resolution Impervious Surface Estimation: An Integration of Ikonos and Landsat-7 ETM+ Imagery, Photogrammetric Engineering & Remote Sensing, 76(12): 1-13.

Nowak, D. J., R. A. Rowntree, E. G. McPherson, S. M. Sisinni, E. R. Kerkmann, and J. C. Stevens, 1996. Measuring and analyzing urban tree cover, Landscape and Urban Planning, 36: 49-57.

Olofsson, P., S. V. Stehman, C. E. Woodcock, D. Sulla-Menashe, A. M. Sibley, J. D. Newell, M. A. Friedl, and M. Herold, 2012. A global land-cover validation data set, part I: fundamental design principles, International Journal of Remote Sensing, 33(18): 5768-5788.

Stehman, S. V., and R. Czaplewski, 1998. Design and analysis for thematic map accuracy assessment: fundamental principles, Remote Sensing of Environment, 64: 331-344.

Stehman, S. V., J. D. Wickham, J. H. Smith, and L. Yang, 2003. Thematic accuracy of the 1992 National Land-Cover Data for the eastern United States: Statistical methodology and regional results, Remote Sensing of Environment, 86: 500-516.

Weng, Q., and X. Hu, 2008. Medium Spatial Resolution Satellite Imagery for Estimating and Mapping Urban Impervious Surfaces Using LSMA and ANN, IEEE Transactions on Geoscience and Remote Sensing, 46(8): 2397-2406.

Wickham, J. D., S. V. Stehman, J. H. Smith, and L. Yang, 2004. Thematic accuracy of the 1992 National Land-Cover Data for the western United States, Remote Sensing of Environment, 91: 452-468.

Wickham, J. D., S. V. Stehman, L. Gass, J. Dewitz, J. A. Fry, and T. G. Wade, 2013. Accuracy assessment of NLCD 2006 land cover and impervious surface, Remote Sensing of Environment, 130: 294-304.

Wu, C., and F. Yuan, 2007. Seasonal Sensitivity Analysis of Impervious Surface Estimation with Satellite Imagery, Photogrammetric Engineering & Remote Sensing, 73(12): 1393-1401.